Research Article | Vol. 26, No. 4 | 19 Feb 2018 | OPTICS EXPRESS 4920
Optics EXPRESS

Fully controllable adiabatic geometric phase in nonlinear optics

AVIV KARNIELI[1,*] AND ADY ARIE[2,3]

[1] *Raymond and Beverly Sackler School of Physics and Astronomy, Tel Aviv University, Ramat Aviv 69978, Tel Aviv, Israel*
[2] *School of Electrical Engineering, Iby and Aladar Fleischman Faculty of Engineering, Tel-Aviv University, Tel-Aviv, Israel*
[3] *Tel Aviv University Center for Light-Matter-Interaction, Tel Aviv 6997801, Israel*
[*] *avivkar1@gmail.com*

Abstract: We propose and analyze a new way for obtaining an adiabatic geometric phase for light, via the sum-frequency-generation nonlinear process. The state of light is represented by the complex amplitudes at two different optical frequencies, coupled by the second order nonlinearity of the medium. The dynamics of this system is then shown to be equivalent to that of a spin-1/2 particle in a magnetic field, which in turn can be rotated adiabatically on the Bloch sphere. When the input wave itself is an eigenstate of the magnetic field equivalent, the geometric phase is manifested as a pure phase factor. Two adiabatic rotation schemes, based on specific modulations of the quasi-phase-matching poling parameters, are discussed. In the first, the geometric phase is shown to be sensitive to the pump intensity variations, as a result of the Bloch sphere deformation. The second can be utilized for the realization of nonlinear-optics-based geometric phase plates. Moreover, non-closed adiabatic trajectories are investigated, which are expected to provide a robust and broadband geometric wavefront shaping in the sum frequency.

OCIS codes: (350.1370) Berry's phase; (090.0090) Holography; (190.0190) Nonlinear optics; (190.2620) Harmonic generation and mixing; (190.4223) Nonlinear wave mixing

References and links

1. S. Pancharatnam, "Generalized theory of interference and its applications," Proc. Ind. Ac. Sci. A. **44**(5), 247-262 (1956).
2. M. V. Berry, "Quantal phase factors accompanying adiabatic changes," Proc. R. Soc. Lond. A, **392**(1802), 45-57 (1984).
3. J. J. Sakurai and J. Napolitano, *Modern quantum mechanics, second edition* (Addison-Wesley, 2011).
4. M. V. Berry, "The adiabatic phase and Pancharatnam's phase for polarized light," J. Mod. Opt. **34**(11), 1401-1407 (1987).
5. J. C. Gutiérrez-Vega, "Pancharatnam-Berry phase of optical systems," Opt. Lett., **36**(7), 1143-1145 (2011).
6. S. Slussarenko, A. Alberucci, C. P. Jisha, S. Fan, B. Piccirillo, E. Santamato, G. Assanto and L. Marrucci, "Guiding light via geometric phases," Nat. Phot., **10**, 571-575 (2016).
7. Z. Bomzon, V. Kleiner and E. Hasman, "Pancharatnam-Berry phase in space-variant polarization-state manipulations with subwavelength gratings," Opt. Lett. **26**(18), 1424-1426 (2001).
8. L. Marrucci, C. Manzo and D. Paparo, "Pancharatnam-Berry phase optical elements for wave front shaping in the visible domain: switchable helical mode generation," App. Phys. Lett **88**, 221102 (2006).
9. M. Khorasaninejad, W. T. Chen, R. C. Devlin, J. Oh, A. Y. Zhu and F. Capasso, "Metalenses at visible wavelengths: Diffraction-limited focusing and subwavelength resolution imaging," Science, **352**(6290), 1190-1194 (2016).
10. R. Y. Chiao and Y. S. Wu, "Manifestations of Berry's topological phase for the photon," Phys. Rev. Lett. **57**(8), 933-936 (1986).
11. A. Tomita and R. Y. Chiao, "Observation of Berry's topological phase by use of an optical fiber," Phys. Rev. Lett. **57**(8), 937-940 (1986).
12. H. Suchowski, D. Oron, A. Arie and Y. Silberberg, "Geometrical representation of sum frequency generation and adiabatic frequency conversion," Phys. Rev. A. **78**, 063821 (2008).
13. H. Suchowski, G. Porat, A. Arie and Y. Silberberg, "Adiabatic processes in frequency conversion," Las. Phot. Rev. **8**(3), 333-367 (2014).
14. H. Suchowski, V. Prabhudesai, D. Oron, A. Arie and Y. Silberberg, "Robust adiabatic sum frequency conversion," Opt. Express **17**(15), 12731-12740 (2009).

#313882 https://doi.org/10.1364/OE.26.004920
Journal © 2018 Received 20 Nov 2017; accepted 27 Dec 2017; published 15 Feb 2018

Optics EXPRESS

15. P. Krogen, H. Suchowski, H. Liang, H. Flemens, K. H. Hong, F. X. Kartner and J. Moses, "Generation and multi-octave shaping of mid-infrared intense single-cycle pulses," Nat. Phot. **11**, 222-226 (2017).
16. C. R. Phillips and M. M. Fejer, "Efficiency and phase of optical parametric amplification in chirped quasiphase-matched gratings," Opt. Lett., **35**(18), 3093-3095 (2010).
17. O. Yaakobi, L. Caspani, M. Clerici, F. Vidal and R. Morandotti, "Complete energy conversion by autoresonant three-wave mixing in nonuniform media," Opt. Express **21**(2), 1623-1632 (2013).
18. P. Mandel, P. Galatola, L. A. Lugiato and W. Kaige, "Berry phase analogies in nonlinear optics," Opt. Comm. **80**(3), 262-266 (1991).
19. M. Tymchenko, J. S. Gomez-Diaz, J. Lee, N. Nookala, M. A. Belkin and A. Alù, "Gradient nonlinear Pancharatnam-Berry metasurfaces," Phys. Rev. Lett. **115**, 207403 (2015).
20. M. Tymchenko, J. S. Gomez-Diaz, J. Lee, N. Nookala, M. A. Belkin and A. Alù, "Advanced control of nonlinear beams with Pancharatnam-Berry metasurfaces," Phys. Rev. B. **94**, 214303 (2016).
21. K. Wang, Y. Shi, A. S. Solntsev, S. Fan, A. A. Sukhorukov and D. N. Neshev, "Non-reciprocal geometric phase in nonlinear frequency conversion," Opt. Lett. **42**(10), 1990-1993 (2017).
22. R. W. Boyd, *Nonlinear optics, third edition* (Academic Press, 2008).
23. A. Shapira, L. Naor and A. Arie, "Nonlinear optical holograms for spatial and spectral shaping of light waves," Sci. Bull. **60**(16), 1403-1415 (2015).
24. S. Trajtenberg-Mills, I. Juwiler and A. Arie, "On-axis shaping of second harmonic beams," Las. Phot. Rev. **9**(6), L40-L44 (2015).
25. J. R. Kurz, A. M. Schober, D. S. Hum, A. J. Saltzman and M. M. Fejer, "Nonlinear physical optics with transversely patterned quasi-phase-matching gratings," J. Sel. Top. Quant. Elect. **8**(3), 660-664 (2002).
26. N. Voloch Bloch, K. Shemer, A. Shapira, R. Shiloh, I. Juwiler and A. Arie, "Twisting light by nonlinear photonic crystals," Phys. Rev. Lett. **108**, 233902 (2012).
27. A. Bahabad and A. Arie, "Generation of optical vortex beams by nonlinear wave mixing", Opt. Express **15**(26), 17619-17624 (2007).
28. M. J. Missey, V. Dominic, L. E. Myers and R. C. Eckardt, "Diffusion-bonded stacks of periodically poled lithium niobate," Opt. Lett. **9**(23), 664-666 (1998).
29. A. Karnieli and A. Arie, "All-optical Stern-Gerlach effect," Phys. Rev. Lett. **120**, 053901 (2018).
30. S. Trajtenberg-Mills and A. Arie, "Shaping light beams in nonlinear processes using structured light and patterned crystals," Opt. Mat. Express **7**(8), 2928-2942 (2017).
31. The specific value of the azimuthal angle of $\hat{n}$ does not play a role in our analysis.

1. Introduction

More than 60 years ago, Pancharatnam [1] pointed out that polarized light can accumulate a phase, in addition to that associated with propagation, when the polarization state is changed over a non-closed trajectory between two points on the Poincare sphere. This *geometric phase* was shown to be calculated via the so called Pancharatnam connection, demonstrating an intrinsic dependence on the geometric properties of the path taken in polarization space. A special case is when the polarization state undergoes a closed trajectory over several points and returns to its original value. The resulting geometric phase, γ, is then associated with the solid angle, Ω, enclosed by the geodesic polygon on the Poincare sphere, namely $\gamma = -\frac{1}{2}\Omega$.

A few decades later, Berry [2, 3] demonstrated that an eigenstate of a quantum-mechanical (QM) Hamiltonian, following an adiabatic closed trajectory in the parameter space, accumulates a geometric phase equal to $\gamma = -\frac{1}{2}\Omega$ for spin-1/2 particles in an adiabatically rotating magnetic field. He later realized [4] that Pancharatnam's phase for polarized light was equivalent to the adiabatic phase for spin-1/2 particles, due to the similar algebra describing the two phenomena. This polarization-induced geometric phase was thereafter called the Pancharatnam-Berry (PB) phase (where the latter is commonly referred to in the context of non-closed trajectories of the polarization state [5]). Indeed, realizations of the PB phase by means of engineered birefringence of optical devices has given rise to numerous applications, such as light guiding [6] and wavefront shaping [7–9].

Chiao et al. [10, 11] have also demonstrated a scheme for the realization of an adiabatic geometric phase for light. They utilized the photon's helicity ($h = \pm 1$) following an adiabatic change in the propagation direction, $\hat{k}$, along a helical fiber with N windings. The resulting geometric phase was then given by $\gamma = \mp N\Omega$, where Ω is now the solid angle enclosed by the trajectory of the k-vector in reciprocal space. The two aforementioned schemes for obtaining

Optics EXPRESS

geometric phases for light are demonstrated in Figs. (1a)-(1b), for the case $\gamma = -\pi$.

In this paper, we introduce a different manifestation of the adiabatic geometric phase for light, that will neither include changes in the polarization nor in the direction of the photons. Rather, we shall harness the equivalence between the dynamics of the nonlinear sum-frequency-generation (SFG) process, and the one describing spin-1/2 particles in a magnetic field. In the presence of an adiabatic rotation of the magnetic field equivalent in parameter space, the two SFG eigenstates, or *mutual beams*, will each acquire a corresponding adiabatic geometric phase. A special case is then considered where the initial eigenstate is the incident wave itself in the idler frequency. The resulting geometric phase is then present in the form of a pure phase factor that can be experimentally measured.

Analogies between SFG and 2-level system dynamics have already given rise to robust, broadband and efficient adiabatic frequency conversion [12–17], where the Hamiltonian was changed adiabatically such that it induces the equivalent of population inversion. Geometric phase analogues have also been studied in nonlinear optics, in the context of four-wave-mixing dynamics [18], as well as with artificially engineered plasmonic metasurfaces [19, 20]. Recently, it was pointed out [21] that a non-adiabatic PB phase exists in the SFG dynamics, thus enabling through unidirectional pumping to realize non-reciprocal propagation, which can be useful for optical isolators. In this paper we focus instead on adiabatic geometric phase analysis. In addition to being robust, the use of adiabatic closed trajectories in parameter space enables the implementation of methods for controlling the geometric phase in nonlinear optics.

The outline of this paper is given as follows: in section 2, we present the theoretical model unveiling the analogy between the spin-1/2 adiabatic geometric phase and the equivalent case in SFG; in section 3, we present different schemes for obtaining and controlling the geometric phase in nonlinear optics; in section 4, we discuss future applications for wavefront shaping, and then finally conclude this paper in section 5.

2. Model

We shall now present the equivalence between spin-1/2 dynamics in a magnetic field and the classical nonlinear optical system. The time-independent coupled wave equations (CWEs) for SFG under the approximations of diffraction-free propagation, slowly varying envelope and undepleted pump field are given by [22]

$$\frac{\partial A_i}{\partial z} = i\frac{2d(z)\omega_i^2}{k_i c^2} A_p^* A_s e^{-i\Delta k_0 z} \tag{1}$$

$$\frac{\partial A_s}{\partial z} = i\frac{2d(z)\omega_s^2}{k_s c^2} A_p A_i e^{i\Delta k_0 z} \tag{2}$$

where A_j with $j = i, p, s$ (for idler, pump and signal, respectively) are the slowly varying envelopes of the interacting waves, z is the propagation coordinate, k_j and ω_j are the wave-numbers and frequencies, respectively, where we set $\omega_s = \omega_i + \omega_p$; $d(z)$ is the spatially varying magnitude of the second-order nonlinear susceptibility, c the speed of light and $\Delta k_0 = k_p + k_i - k_s$ is the phase mismatch. For increasing conversion efficiency, the nonlinear susceptibility can be periodically modulated in order to compensate for the phase mismatch, a technique known as quasi phase matching QPM [22]. If an adiabatic modulation is subjected on the QPM parameters, we can describe the nonlinear coefficient as a Fourier series with slowly varying components,

$$d(z) = d_{ij} \sum_{m=-\infty}^{\infty} |d_m(z)| \exp\left\{ im\left[\int_0^z q(z')dz' + \phi_d(z) \right] \right\}, \tag{3}$$

where for $m \neq 0$, $|d_m(z)| = (2/m\pi)\sin(m\pi D(z))$, with $0 \leq D(z) \leq 1/2$ being the duty cycle of the modulation, and $|d_0(z)| = 2D(z) - 1$, $q(z)$ is the modulation wave-vector, $\phi_d(z)$ the modulation phase, and d_{ij} is the corresponding component of the nonlinear susceptibility tensor.

Optics EXPRESS

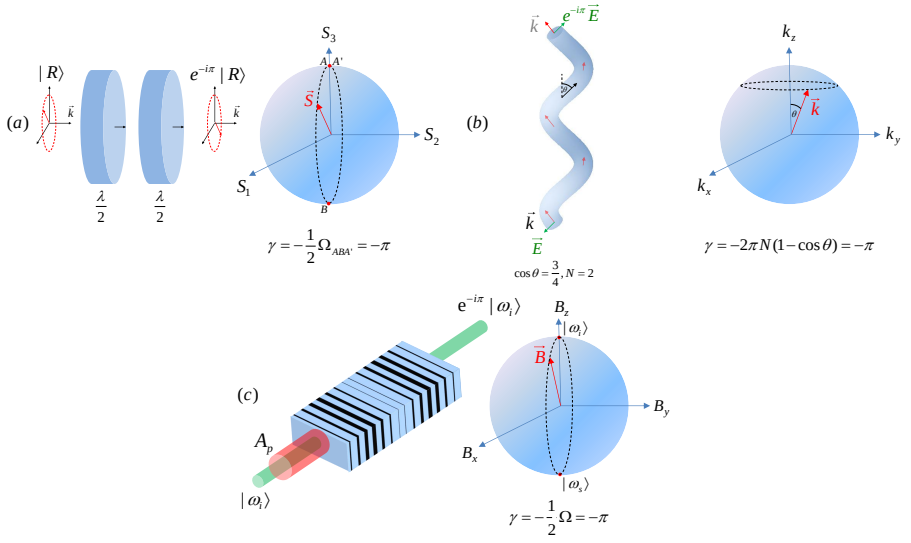

Fig. 1. Different schemes for obtaining a geometric phase of $\gamma = -\pi$ for light. (a) The closed-trajectory Pancharatnam-Berry phase: a circularly-polarized light beam undergoes subsequent birefringence via 2 half-wavelength plates, enclosing a solid angle $\Omega = 2\pi$ on the Poincare sphere, and where $\gamma = -\frac{1}{2}\Omega$. (b) The adiabatic geometric phase for the photon helicity. A guided mode experiences an adiabatic change in direction when it propagates along a helical fiber with $N = 2$ windings. This path encloses a solid angle $\Omega = \pi/2$ on the k-vector sphere, where now $\gamma = -N\Omega$. (c) The adiabatic nonlinear optical geometric phase. A mutual beam eigenstate in the idler frequency, $|\omega_+\rangle = |\omega_i\rangle$, follows a closed trajectory of the magnetic field equivalent on the SFG sphere, enclosing a solid angle $\Omega = 2\pi$, where $\gamma = -\frac{1}{2}\Omega$. The closed trajectory is enabled through a specific modulation of the QPM parameters: the phase mismatch and poling duty cycle.

Substituting Eq. (3) into Eqs. (1) and (2), we keep in the right hand side only one of the terms $m = \pm 1$ which are assumed to oscillate closest to phase matching, similar to the rotating wave approximation. Next, we make a transformation to a rotating frame $(\tilde{A}_i, \tilde{A}_s)$ given by

$$A_i = \sqrt{k_s}\omega_i \exp\left\{-\frac{i}{2}\left[\Delta k_0 z - \int_0^z q(z')dz'\right]\right\}\tilde{A}_i, \tag{4}$$

$$A_s = \sqrt{k_i}\omega_s \exp\left\{\frac{i}{2}\left[\Delta k_0 z - \int_0^z q(z')dz'\right]\right\}\tilde{A}_s. \tag{5}$$

Finally, we denote $A_p = |A_p|e^{i\phi_p} \equiv const$, $d_{eff} = (2/\pi)d_{ij}$ and $\bar{d} = \sin[\pi D(z)]$ as the normalized first-order QPM modulation strength, and introduce the dimensionless time coordinate $\tau = \sqrt{k_i k_s}z$. We can now use these definitions to rewrite the CWEs as a single matrix equation,

$$i\frac{\partial}{\partial\tau}\begin{pmatrix}\tilde{A}_i\\ \tilde{A}_s\end{pmatrix} = -\sigma\cdot\mathbf{B}(\tau)\begin{pmatrix}\tilde{A}_i\\ \tilde{A}_s\end{pmatrix}, \tag{6}$$

where $\sigma = (\sigma_x, \sigma_y, \sigma_z)$ is the Pauli matrix vector [3]. Here the optical equivalent of the time-dependent magnetic field is given by

$$\mathbf{B}(\tau) = B_0(\tau)\hat{\mathbf{B}}[\theta(\tau), \phi(\tau)], \tag{7}$$

where $\hat{\mathbf{B}}$ is a unit vector, possessing the spherical angles $\theta(\tau)$ and $\phi(\tau)$, and $B_0(\tau)$ defines the field's magnitude. These quantities can be expressed as functions of the QPM modulation

Optics EXPRESS

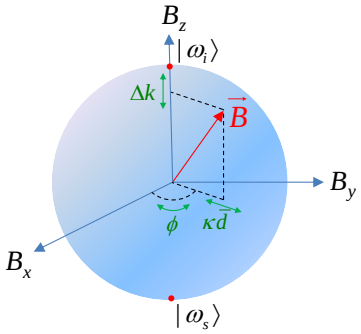

Fig. 2. The control over the equivalent magnetic field is possible via the variation of the QPM parameters. The $\hat{z}$ component of $\mathbf{B}$ is proportional to the phase mismatch Δk, the transverse radial component is given by the product of the nonlinear coupling κ and duty cycle parameter $\bar{d}$, and the relative phase between the pump and the poling pattern, ϕ, determines the azimuthal angle.

parameters, such that

$$B_0(\tau) = \frac{1}{2\sqrt{k_i k_s}}\sqrt{\kappa^2\bar{d}^2(\tau) + \Delta k^2(\tau)}, \tag{8}$$

$$\cos\theta(\tau) = \frac{\Delta k(\tau)}{\sqrt{\kappa^2\bar{d}^2(\tau) + \Delta k^2(\tau)}}, \tag{9}$$

$$\phi(\tau) = \phi_p - \phi_d(\tau). \tag{10}$$

In the above equations, we have introduced the nonlinear coupling $\kappa = 4|d_{eff}A_p|\sqrt{k_i k_s}/n_i n_s$ and the total phase mismatch $\Delta k(\tau) = \Delta k_0 - q(\tau)$, where $n_j = n(\omega_j)$ is the frequency-dependent refractive index of the medium. As can be seen from Eqs. (7)-(10), the z component of the magnetic field equivalent is proportional to the phase-mismatch Δk, namely $B_z = \Delta k/(2\sqrt{k_i k_s})$; the magnitude of its transverse component, $\mathbf{B}_T = \hat{x}B_x + \hat{y}B_y$, satisfies $|\mathbf{B}_T| = \kappa\bar{d}/(2\sqrt{k_i k_s})$, and the direction of this component is determined by the phase ϕ. It is evident that the field's magnitude and direction are fully controllable via the QPM modulation's period, duty cycle and phase. Fig. (2) illustrates this observation.

The vector $(\tilde{A}_i \quad \tilde{A}_s)^T$ can be described as a state vector using spin-1/2 nomenclature. Adopting the braket notation, we write this state as $|\psi\rangle = \left(\tilde{A}_i|\omega_i\rangle + \tilde{A}_s|\omega_s\rangle\right)/\sqrt{|\tilde{A}_i|^2 + |\tilde{A}_s|^2}$, where $|\tilde{A}_i|^2 + |\tilde{A}_s|^2 = const.$, due to the Manley-Rowe relations [22]. Different frequency kets $|\omega_j\rangle$ are orthogonal in the sense that they cannot produce an observable interference intensity pattern, and they are also distinguishable by means of spectral filtering. Explicitly, if different carrier frequencies are assumed to be located far apart (with respect to their bandwidth) in the spectral domain, we can write $\langle\omega_j|\omega_k\rangle = \int d\omega' S_j^*(\omega')S_k(\omega') = \delta_{jk}$. In the latter relation, $S_j(\omega') \equiv \langle\omega'|\omega_j\rangle$ is the normalized ($\int d\omega'|S(\omega')|^2 = 1$) spectral amplitude of the $|\omega_j\rangle$ wave, at frequency ω'.

We call the state $|\psi\rangle$ a *mutual beam*, since it comprises of two co-propagating frequency components. The ket states $|\omega_i\rangle$ and $|\omega_s\rangle$ can be identified as the equivalents of the spin-up $|\uparrow_z\rangle$ and spin-down $|\downarrow_z\rangle$ in the z-basis of the spin, respectively. All the possible states of the system can now be mapped onto a Bloch sphere, with the spin-up (idler wave) and spin-down (signal wave) states located at the north and south poles of the sphere, respectively. In that sense, we can interpret this representation of the state of light as a new type of polarization, namely *spectral polarization*.

Elementary QM dictates that two mutual beam eigenstates of the Hamiltonian $H = -\sigma \cdot \mathbf{B}$

Optics EXPRESS

correspond to a magnetic field equivalent in the direction $\hat{\mathbf{B}}$. These eigenstates are given by

$$|\omega_+\rangle = \cos\frac{\theta}{2}|\omega_i\rangle + e^{i\phi}\sin\frac{\theta}{2}|\omega_s\rangle, \tag{11}$$

$$|\omega_-\rangle = \sin\frac{\theta}{2}|\omega_i\rangle - e^{i\phi}\cos\frac{\theta}{2}|\omega_s\rangle, \tag{12}$$

whereas the dynamics of the total state will be expressed as $|\psi\rangle = \tilde{A}_+(0)e^{iB_0\tau}|\omega_+\rangle + \tilde{A}_-(0)e^{-iB_0\tau}|\omega_-\rangle$. Namely, the state vector precesses about the vector $\hat{\mathbf{B}}$ on the Bloch sphere.

Now, if the direction of the magnetic field equivalent was to be changed adiabatically round a closed trajectory in parameter space, i.e. $\hat{\mathbf{B}} = \hat{\mathbf{B}}(\tau)$, each eigenstate would have accumulated a geometric phase, $\gamma_\pm$, in addition to the dynamic phase $B_0\tau$, such that

$$|\psi\rangle = \tilde{A}_+(0)e^{i\gamma_+}e^{iB_0\tau}|\omega_+\rangle + \tilde{A}_-(0)e^{i\gamma_-}e^{-iB_0\tau}|\omega_-\rangle. \tag{13}$$

By virtue of Berry's result for spin-1/2 [2], we identify

$$\gamma_\pm = \mp\frac{1}{2}\Omega. \tag{14}$$

where Ω is the solid angle enclosed by the trajectory of $\hat{\mathbf{B}}$ in parameter space.

The geometric phase is manifested as a pure phase factor only if the system was initially at an eigenstate of the $\hat{\mathbf{B}}$ direction [Eqs. (11)-(12)]. In the case where only an idler wave is incident on a non-linear crystal at $\tau = 0$, i.e. $|\psi(0)\rangle = |\omega_i\rangle$, this means that the trajectory of the magnetic field equivalent needs to start (and end) with $\hat{\mathbf{B}} = \hat{z}$. As a consequence, the corresponding schemes for the rotation of $\mathbf{B}$ should involve a simultaneous adiabatic change in both angles θ and ϕ (and, for now, keeping B_0 constant). Fortunately, these schemes can be specifically tailored since, as we explained previously, the magnetic field analogue is fully controllable. For the discussed case where $|\psi(0)\rangle = |\omega_i\rangle$ and $\hat{\mathbf{B}}(0) = \hat{\mathbf{B}}(T) = \hat{z}$ ($T = \sqrt{k_i k_s}L$ is the adiabatic rotation period and where L is the crystal length), we obtain in the laboratory (non rotating) frame

$$|\psi(T)\rangle = \exp\left(i\varphi_D + i\gamma_+\right)|\omega_i\rangle. \tag{15}$$

In the above equation, the dynamic phase term, φ_D, is given by $\varphi_D = B_0T - \langle B_z\rangle T$, where

$$\langle B_z\rangle = \frac{1}{T}\int_0^T \frac{\Delta k(\tau)}{2\sqrt{k_i k_s}}d\tau \tag{16}$$

is the average value of the z-component of the field over the adiabatic rotation. The expression (16) is present due to the transformation, Eqs. (4)-(5), applied in the derivation of the dynamical equation, Eq. (6). Once the dynamic phase is eliminated, the pure geometric phase term can be measured. The simplest experimental set-up for measuring the geometric phase takes the form of a Mach-Zehnder interferometer, as depicted in Fig. (3). One arm of the interferometer experiences a phase delay of $\varphi_D + \gamma_+$ due to a poled nonlinear crystal inducing the geometric phase γ_+ on an incident idler wave. In the second arm, an identical crystal is situated such that the poling structure is oppositely oriented with respect to the propagation axis. Due to the geometric nature of the adiabatic phase, the phase delay in the second arm is given by $\varphi_D - \gamma_+$. As the two idler fields interfere, the resulting intensity at the interferometer's output will be given by $I_{tot} = 4I_0\sin^2\gamma_+$. Utilizing this simple interference pattern, the dependence of the purely-geometric phase on the different physical parameters of the system can be studied in a straightforward manner.

Optics EXPRESS

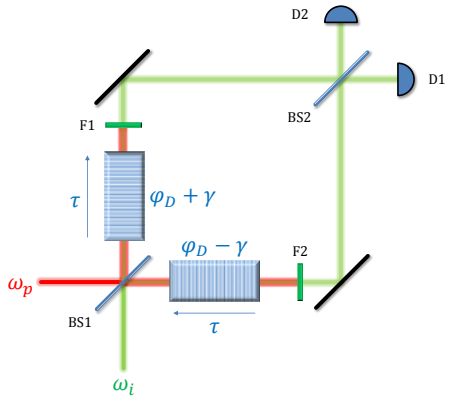

Fig. 3. Mach-Zehnder interferometric setup for measuring the geometric phase, consisting of symmetric beam splitters (BS1-2), filters (F1-2) and detectors (D1-2). The pump and idler beams mix in the different arms of the interferometer. Two identical geometric-phase-inducing nonlinear crystals are situated in each arm with oppositely oriented poling patterns with respect to the propagation axes. Due to its geometric properties, the phase difference between the two arms equals twice the geometric phase.

3. Schemes for adiabatic rotations

In this section we present two different schemes for adiabatic rotations of the magnetic field equivalent, yielding a desired geometric phase. The first involves a circular trajectory about a pre-defined unit vector, while the second is realized by an adiabatic path enclosing a wedge of the unit sphere, which can also be generalized to non-closed trajectories. We then describe the geometric robustness of the second scheme, and discuss the possibilities for optical controllability of the geometric phase, present in the first scheme, via the pump intensity.

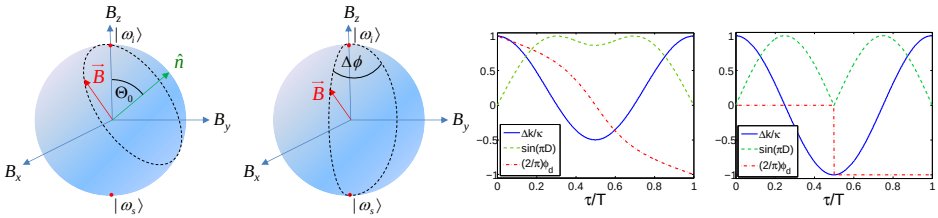

Fig. 4. Schemes for adiabatic rotations on the SFG sphere inducing a geometric phase for the idler wave. (a) Circular adiabatic rotation: the magnetic field equivalent precesses about some unit vector $\hat{n}(\Theta_0)$. (b) Wedged adiabatic rotation: the trajectory of the field encloses a wedge of the unit sphere with opening angle $\Delta\phi$. (c)-(d) Normalized QPM modulation parameters corresponding to the circular (with $\Theta_0 = \pi/3$) and wedged (with $\Delta\phi = \pi/2$) rotation schemes, respectively.

3.1. Circular adiabatic rotation

The general parametrization with respect to τ of a circular trajectory of the magnetic field equivalent, rotating in a CCW fashion about some unit vector $\hat{n}(\Theta_0)$ (Θ_0 is the angle with respect to the z-axis [31]) with frequency ω_0 and starting at $\hat{z}$, is given by

$$\cos\theta(\tau) = \sin^2\Theta_0 \cos\omega_0\tau + \cos^2\Theta_0, \tag{17}$$

Optics EXPRESS

$$\phi(\tau) = -\arctan\frac{\sin\omega_0\tau}{\cos\Theta_0(1-\cos\omega_0\tau)}. \tag{18}$$

This type of trajectory in the parameter space is illustrated in Fig. (4a). The parametrization given by Eqs. (17)-(18) is readily realized by the choice of the proper QPM modulation parameters:

$$\Delta k(\tau) = \kappa(\sin^2\Theta_0\cos\omega_0\tau + \cos^2\Theta_0), \tag{19}$$

$$D(\tau) = \frac{1}{\pi}\arcsin\sqrt{1-(\sin^2\Theta_0\cos\omega_0\tau + \cos^2\Theta_0)^2}, \tag{20}$$

$$\phi_d(\tau) = \phi_p + \arctan\frac{\sin\omega_0\tau}{\cos\Theta_0(1-\cos\omega_0\tau)}. \tag{21}$$

and $\omega_0 = 2\pi/T$, ensuring a single full rotation of the Hamiltonian. Figure (4c) demonstrates the required modulation. The resulting geometric phase of the above scheme is given by

$$\gamma_+ = -\pi(1-\cos\Theta_0), \tag{22}$$

where as the dynamic phase equals to [see Eqs. (8), (13) and (19)]

$$\varphi_D = B_0T - \langle B_z\rangle T = \frac{1}{2}\kappa L\sin^2\Theta_0. \tag{23}$$

To illustrate the effect of the adiabatic trajectory on the SFG process, we solve numerically the dynamical equations, Eqs. (1)-(2), in the presence of the QPM modulation given by Eqs. (3) and (19)-(21). The idler, signal and pump wavelengths were chosen as $\lambda_i = 600$ nm, $\lambda_s = 432.6$ nm and $\lambda_p = 1550$ nm, respectively. The idler wave is incident on a 2.5 cm long nonlinear $LiNbO_3$ crystal with $d_{eff} = 17.2$pm/V, pumped with a uniform intensity of $I_p = 100$ MW/cm^2. Fig. (5a) shows the normalized photon numbers of the idler and signal waves, given by $N_{i,s} \equiv |A_{i,s}|^2/\sqrt{|A_i|^2+|A_s|^2}$, as well as the accumulation of the geometric phase, along the propagation coordinate z, for $\Theta_0 = \pi/3$. It is found that the normalized photon number of the idler wave is reduced to $1/4$ midway of the crystal, while the signal photon number is simultaneously increased to $3/4$. This is an indication that the state traverses the point on the sphere corresponding to $2\Theta_0 = 2\pi/3$. Furthermore, the accumulated geometric phase is in good agreement with Eq. (22).

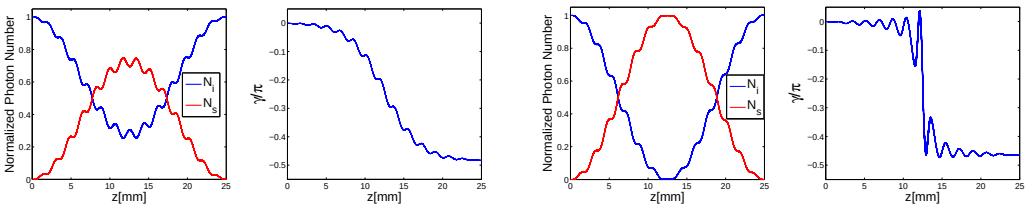

(a) (b)

Fig. 5. Simulations of the normalized photon numbers of the idler and signal waves (left) and geometric phase accumulation (right) along the propagation coordinate z. (a) Results for the circular adiabatic rotation scheme with $\Theta_0 = \pi/3$, and thus $\gamma_+ = -\pi/2$. (b) Results for the wedged adiabatic rotation with $\Delta\phi = \pi/2$, giving $\gamma_+ = -\pi/2$.

3.2. *Wedged adiabatic rotation*

A dependence of the dynamic phase on geometric parameters, such as the one present in Eq. (23), is less desirable when one considers the design of purely-geometric phase-plates. The

Optics EXPRESS

latter rely on the transverse modulation of the geometric phase's value, resulting in a shaped phase-front, insensitive of the path length. This is not easily achieved if the dynamical phase is also transversely-variant. Therefore, a scheme where the average z-component of the magnetic field equivalent vanishes (i.e., $\langle B_z \rangle = 0$) is desirable, yielding $\varphi_D = B_0 T$ irrespective of the transverse coordinates. This type of scheme is readily given by

$$\cos\theta(\tau) = \cos\omega_0\tau, \tag{24}$$

$$\phi(\tau) = H\left(\tau - \frac{T}{2}\right)\Delta\phi, \tag{25}$$

where in Eq. (25), $H(\tau)$ is the Heaviside step-function. This trajectory is illustrated in Fig. (4b). The field follows an adiabatic rotation along a great circle from the north pole to the south pole of the SFG sphere. The angle ϕ is then rotated by an amount $\Delta\phi$, and then the field is rotated back towards the north pole. The resulting path of the field encloses a wedge of the SFG sphere corresponding to a solid angle of $\Omega = 2\Delta\phi$, and the emergent geometric phase for the idler wave is

$$\gamma_+ = -\Delta\phi. \tag{26}$$

The parametrization of the QPM modulation parameters for this scheme is

$$\Delta k(\tau) = \kappa\cos\omega_0\tau \tag{27}$$

$$D(\tau) = \frac{1}{\pi}\arcsin|\sin\omega_0\tau|, \tag{28}$$

$$\phi_d(\tau) = \phi_p - H\left(\tau - \frac{T}{2}\right)\Delta\phi, \tag{29}$$

as shown in Fig. (4d). We repeat the numerical calculations with the same physical parameters as before, however this time in the presence of the QPM modulation given by Eqs. (27)-(29), and for $\Delta\phi = \pi/2$. Fig. (5b) shows that the normalized photon number of the idler wave is reduced to 0 midway of the crystal, while the signal photon number is simultaneously increased to 1, as expected for this trajectory, traversing the south pole of the SFG sphere. It appears that the accumulated geometric phase experiences a discontinuity near the south pole. However, the geometric phase at the end of the adiabatic rotation is still in good agreement with Eq. (26).

3.3. Geometric phase robustness and pump-controlled phase shifts

In the aforementioned schemes, it was assumed that the input pump intensity I_p corresponds to the specific value of κ used in the QPM poling pattern, in either Eq. (19) or Eq. (27). Under this assumption, the vector $\mathbf{B}$ remains on the surface of the Bloch sphere [see Eq. (8) for the magnitude of the magnetic field equivalent]. We now investigate how a different input pump intensity I_p' affects our derivations and, more interestingly, controls the geometric phase. For convenience, we shall keep the notation κ and I_p as the a-priori selected coupling and intensity values used in the poling pattern of $\Delta k(\tau)$. The input value of the pump intensity, I_p', will correspond to a different coupling value denoted as κ'. This change can only affect the x, y-components of the magnetic field equivalent by virtue of Eqs. (7)-(10). Explicitly, we now have

$$\mathbf{B}(\tau) = \tilde{B}_0\left[\eta\sin\alpha(\tau)\hat{\rho}(\tau) + \cos\alpha(\tau)\hat{z}\right], \tag{30}$$

where $\eta = \sqrt{I_p'/I_p}$, $\tilde{B}_0 = \kappa/2\sqrt{k_i k_s}$, $\hat{\rho}(\tau) = \hat{x}\cos\phi(\tau) + \hat{y}\sin\phi(\tau)$, and $\cos\alpha(\tau) = \sin^2\Theta_0\cos\omega_0\tau + \cos^2\Theta_0$ or $\cos\alpha(\tau) = \cos\omega_0\tau$ for the circular and wedged schemes, respectively. It is clear now that for a different pump intensity, the trajectory of $\mathbf{B}$ now lies on the

Optics EXPRESS

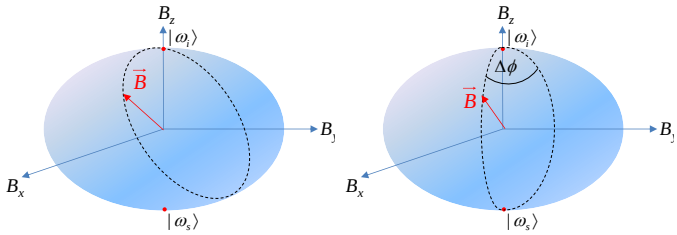

Fig. 6. Adiabatic rotations on the Bloch spheroid for $\eta > 1$. (a) For the circular adiabatic rotation, the trajectory of the field is no longer described by a simple rotation about a constant unit vector. The flux through the surface enclosed by the field's rotation is different than for the same parametrization on the Bloch sphere ($\eta = 1$). (b) From symmetry considerations, in case of wedged adiabatic rotation the field's trajectory encloses the same wedge as if it were on the unit sphere, retaining the value of the geometric phase.

surface of a spheroid (either oblate or prolate, depending on η). Figure (6) depicts this scenario for the two adiabatic rotation schemes.

The simplest way to calculate the geometric phase now is to consider the Berry connection $\mathbf{A}(\mathbf{B})$, given by [3]

$$\mathbf{A}(\mathbf{B}) = i\,\langle\omega_+;\tau|\nabla_{\mathbf{B}}|\omega_+;\tau\rangle = -\hat{\phi}\frac{1-\cos\theta}{2|\mathbf{B}|\sin\theta}. \tag{31}$$

The geometric phase is then given in terms of the Berry connection by

$$\gamma_+ = \oint \mathbf{A}(\mathbf{B})\cdot d\mathbf{B} = -\frac{1}{2}\int_0^T (1-\cos\theta)\dot{\phi}\,d\tau, \tag{32}$$

where $\dot{\phi} = d\phi/d\tau$, and

$$\cos\theta = \frac{\mathbf{B}\cdot\hat{z}}{|\mathbf{B}|} = \frac{\cos\alpha}{\sqrt{\eta^2\sin^2\alpha+\cos^2\alpha}}. \tag{33}$$

Remarkably, it is straightforward to see from symmetry considerations of Gauss's theorem that the geometric phase of the wedged adiabatic rotation is invariant under changes in the pump intensity [Fig. (4b)]. Alternatively, this can be shown via inserting $\dot{\phi} = \Delta\phi\delta(\tau - T/2)$ and $\cos\alpha = \cos\omega_o\tau$ in Eqs. (32)-(33), and finding $\gamma_+ = -\Delta\phi$, independent of η. As this scheme might be utilized for geometric phase plates, this invariance under the pump intensity is highly desirable.

Moreover, it can be concluded that this scheme may be generalized to a wedged trajectory on an *arbitrary* surface, provided that the latter has rotational symmetry with respect to the z axis. We remark that the Berry flux, which determines the geometric phase, through a $\Delta\phi$-wedge of all rotationally-symmetric surfaces is identical, given that they enclose the origin of parameter space. It is apparent, therefore, that the only condition for the validity of the wedged adiabatic rotation scheme is inherently geometric: all wedge trajectories must lie on a rotationally symmetric surface enclosing the origin. The origin, in turn, lies inside the surface for a relatively wide range of pump wavelengths. This observation ensures that the wedged rotation scheme is broadband, a property also exhibited by adiabatic frequency conversion processes [12].

We now turn our attention to the second rotation scheme, the circular adiabatic rotation. In this case, the change in pump intensity induces a change in the geometric phase given by

$$\Delta\gamma_+(\eta,\Theta_0) = -\frac{\cos\Theta_0}{2}\int_0^{2\pi} f(\eta,\cos\alpha)\frac{\cos\alpha}{1+\cos\alpha}d\beta, \tag{34}$$

Optics EXPRESS

where $\beta = \omega_0 \tau$ and

$$f(\eta, \cos\alpha) = 1 - \frac{1}{\sqrt{\eta^2 + (1-\eta^2)\cos^2\alpha}}. \tag{35}$$

If we consider small changes in η around unity, i.e. $\eta = 1 + \epsilon$ where $\epsilon \ll 1$, then $f \simeq \epsilon \sin^2\alpha$, and we find

$$\frac{d\gamma_+}{d\epsilon} = \gamma_+^{(0)} \cos\Theta_0 (1 + \cos\Theta_0) \left(\frac{3}{2}\cos^2\Theta_0 - \frac{1}{2} \right), \tag{36}$$

where $\gamma_+^{(0)} = -\pi(1 - \cos\Theta_0)$. This purely-geometric phase shift might be measurable via the Mach-Zehnder interferometer, as discussed in section 2. The resulting geometric phase can be viewed as being optically-controlled by the pump wave; this in turn may open doors to novel applications requiring this feature.

3.4. Non-closed trajectories

As it turns out, a manifestation of the PB phase can readily be recognized if one considers the corresponding phenomena in light polarization. A broadly used scheme for PB optical elements relies on the SU(2) rotations imposed by a half wave plate (HWP) with angle α between the optical axis and the x-axis. The eigenvectors of this HWP lie on the equator of the Poincare sphere. A left circularly polarized (LCP) state, positioned on the north pole, is rotated by the HWP about the axis spanned by its eigenvectors, until it reaches the south pole, namely the right circular polarization (RCP). Denoting $\phi = 2\alpha$ as the corresponding azimuthal angle of the axis of rotation on the Poincare sphere, the resulting state is given by $\exp(i\phi)\,|R\rangle$. The phase ϕ is then interpreted as the PB phase acquired by the state. When ϕ is transversely varied, i.e. $\phi = \phi(x, y)$, the resulting wavefront is said to be shaped via the geometric phase.

A similar treatment can be utilized in SFG dynamics. The main difference is, that in the general case the SFG Hamiltonian itself can induce a HWP-like rotation. To see this, we consider the fundamental solution to the SFG dynamics with vanishing phase mismatch ($\cos\theta = 0$) and an incident idler wave,

$$|\psi(\tau)\rangle = \cos B_0\tau\,|\omega_i\rangle + i\exp(i\phi)\sin B_0\tau\,|\omega_s\rangle\,. \tag{37}$$

At time $\tau_0 = \pi/2B_0$, the resulting state (up to a constant phase factor) is $|\psi(\tau_0)\rangle = \exp(i\phi)\,|\omega_s\rangle$. Namely, the input idler state has transformed into a signal wave ket with a controllable geometric phase ϕ. This scheme, inherent to the SFG dynamics, has been utilized in the past for wavefront shaping of up-converted light beams [23–25], though it has yet to be interpreted in a geometric context. However, it is not as robust as the PB scheme for polarized light, since the magnitude of the resulting signal wave is dependent on the specific value of the pump intensity that is necessary for converting the idler wave into the signal wave. To achieve conversion robustness, an adiabatic scheme is preferred. For this we consider the non-gauge-invariant form of the geometric phase [3] given in terms of the Berry connection, accumulated by the wavefront on a specific point (x, y),

$$\gamma_+[\phi(x,y)] = \int_{|\omega_i\rangle}^{|\omega_s\rangle} \mathbf{A}\left\{\mathbf{B}[\phi(x,y)]\right\} \cdot d\mathbf{B}. \tag{38}$$

In the above equation, $\mathbf{B}[\phi(x, y)]$ is the adiabatic trajectory of the field for the point (x, y) on the wavefront. This field follows half a great circle from the north to the south pole, with a constant azimuthal angle $\phi(x, y)$. As a result, two different points on the wavefront are expected to display different non-gauge-invariant geometric phases given by Eq. (38).

However, by virtue of our result for the wedged adiabatic rotation [Eq. (26) and Fig. (4b)], we find that the geometric phase *difference* $\Delta\phi$ between two points on the wavefront is a well defined quantity, as the latter equals the gauge-invariant closed path integral. As in the case of

Optics EXPRESS

polarization-based PB optical elements, the local phase $\phi(x, y)$ can be controlled, allowing for robust and broadband wavefront geometric phase shaping in the sum-frequency.

We conclude this section with a reminder that all the above analysis is also applicable to the case where the incident wave is in the signal frequency, i.e. $|\psi(0)\rangle = |\omega_s\rangle$. The accumulated phase of this eigenstate of the SFG Hamiltonian then becomes $\gamma_- = -\gamma_+$. Thus, every geometric phase effect induced on the idler wave has a conjugate effect on the signal wave. Examples of this feature will be discussed below.

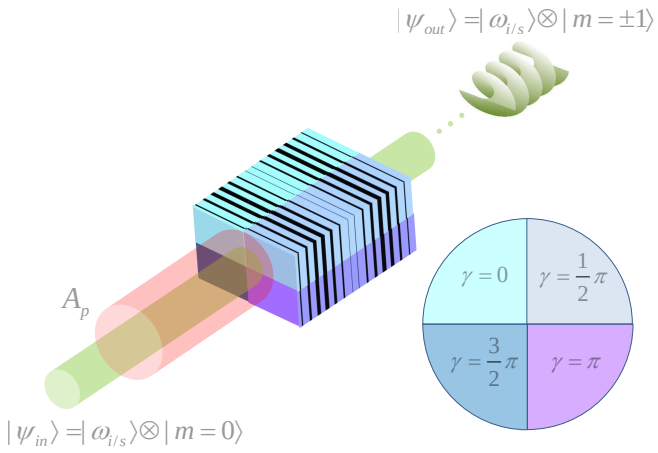

Fig. 7. A vortex beam geometric phase plate. Four GPNLCs with clockwise increasing geometric phase constitute the apparatus. An incident idler beam is expected to accumulate an OAM quantum number of $m = 1$ in the far-field, whereas an incident signal beam accumulates $m = -1$.

4. Future prospects for wavefront shaping

Future applications of nonlinear geometric phase plates in the scope of current technological capabilities include one dimensional (1D) wavefront shaping and manipulation, in a similar manner to the PB-based linear wavefront shapers that rely on polarization [7, 8]. For example, a Gaussian beam can be approximately transformed into a Hermite-Gaussian (HG) mode of order (n0) [or (0n)] where n is the number of nodes in the wavefront. This can be done via an array of $n + 1$, $\gamma = \pi/2$ geometric phase nonlinear crystals (GPNLCs) with alternating directionality, generating a wavefront with an alternating phase. In the far field, such a wavefront is expected to approach an HG-(n0) beam.

Another example is a cylindrical geometric phase lens [9], implemented via encoding a continuous, quadratic variation of γ along one transverse direction. If an incident idler beam is expected to accumulate a converging parabolic phase, then such a lens will be converging for the idler wave and diverging for the signal wave. Additionally, flipping the directionality of the lens renders it diverging for the idler wave, and converging for the signal wave. This feature can be attributed to the geometric nature of the lens.

Advancements in the manufacturing technology of 3D nonlinear photonic crystals may open possibilities for 2D wavefront shaping as implemented today by polarization-based geometric phase plates. One application, amongst numerous others, is the nonlinear shaping of beams with orbital angular momentum (OAM) [26, 27], also known as vortex beams. The simplest scheme for such a realization which does not include a complex, continuous variation of the geometric phase is presented in Fig (7). A Gaussian beam (with zero OAM) is incident on four GPNLCs

Optics EXPRESS

with phases $\gamma = 0, \pi/2, \pi$ and $3\pi/2$ that are placed as a 2×2 matrix, where the phase increases in a clockwise fashion. In the far-field, the resulting idler wave is expected to obtain an OAM of value $+\hbar$. A complementary angular momentum of $-\hbar$ is expected to be obtained by illuminating the crystal with a signal wave, instead of an idler wave. This nonlinear shaper can actually be realized by diffusion bonding [28] of two GPNLC plates, each containing two different phases.

The concept of beam shaping can be further extended, beyond the simple examples given above, to realize optically controlled geometric phase holograms, that enable arbitrary shaping of the wavefront by the nonlinear process.

5. Summary and conclusions

In summary, we have proposed and analyzed new ways for obtaining an adiabatic geometric phase for light, via nonlinear interactions. In principle, this scheme is similar to the closed-trajectory version of the PB phase for polarized light. However, whereas light polarization is defined by two complex amplitudes at two orthogonal directions, here we have harnessed a new degree of freedom - the spectral polarization. This type of polarization is represented by the complex amplitudes at two different optical frequencies, that are coupled by the second order nonlinearity of the medium. Consequently, the spectral polarization eigenstates, or mutual beams, can serve as a new basis for describing the state of light [29].

The proposed adiabatic geometric phase in nonlinear optics might as well open doors for new applications. Since the geometric phase can in principle be designed to take different values as a function of the transverse coordinates, it enables new and exciting possibilities for nonlinear beam shaping and nonlinear holography [30]. Furthermore, the geometric phase shift due to the deformation of the Bloch sphere can be further studied either from a fundamental viewpoint or for the realization of an optically-controlled geometric phase. We are hopeful that this new perspective will eventually lead to novel applications for geometric phases in particular, and nonlinear optics in general, both in the classical and quantum domains.

A. Appendix: the adiabatic condition

Indeed, the adiabaticity of the aforementioned schemes for obtaining the geometric phase in nonlinear optics requires that the time scale τ_0 for changes in $\hat{\mathbf{B}}$ must be larger than the period of the dynamic phase. We can write explicitly [3]

$$\frac{1}{\tau_0} \equiv \frac{\langle \omega_- | \dot{H} | \omega_+ \rangle}{E_+ - E_-} \ll E_+. \tag{39}$$

where $\dot{H}$ is the time derivative of the Hamiltonian, and $E_\pm$ are the energy eigenvalues. In our context, $E_\pm = \mp B_0$ and $\langle \omega_- | \dot{H} | \omega_+ \rangle = B_0 \omega_0$. The adiabatic condition then reduces to $\omega_0 \ll 2B_0$, and in terms of the parameters of the optical system it is given by $L \gg \Lambda$, where

$$\Lambda \equiv \frac{2\pi}{\kappa} = \frac{\pi n_i n_s}{2|d_{eff} A_p| \sqrt{k_i k_s}} \tag{40}$$

is the adiabaticity length scale of the problem. Evidently, the pump field and crystal length have to take values in excess of $100\mathrm{MW/cm}^2$ and a few millimeters, respectively, to satisfy this condition for $\lambda = 500\mathrm{nm}$. These values can be obtained fairly easily with Q-switched solid state pump lasers and ferroelectric nonlinear crystals like $LiNbO_3$ or $KTiOPO_4$.

Funding

Israel Science Foundation (1415/17).